BULLETIN OF THE POLISH ACADEMY OF SCIENCES
TECHNICAL SCIENCES, Vol. 71(5), 2023, Article number: e145763
DOI: 10.24425/bpasts.2023.145763

CONTROL, INFORMATICS AND ROBOTICS

Model predictive ship trajectory tracking system based on line of sight method

Anna MILLER*

Gdynia Maritime University, ul. Morska 81-87, 81-225 Gdynia, Poland

Abstract. Maritime Autonomous Surface Ships (MASS) perfectly fit into the future vision of merchant fleet. MASS autonomous navigation system combines automatic trajectory tracking and supervisor safe trajectory generation subsystems. Automatic trajectory tracking method, using line-of-sight (LOS) reference course generation algorithm, is combined with model predictive control (MPC). Algorithm for MASS trajectory tracking, including cooperation with the dynamic system of safe trajectory generation is described. It allows for better ship control with steady-state cross-track error limitation to the ship hull breadth and limited overshoot after turns. In real MASS ships path is defined as set of straight line segments, so transition between trajectory sections when passing waypoint is unavoidable. In the proposed control algorithm LOS trajectory reference course is mapped to the rotational speed reference value, which is dynamically constrained in MPC controller due to dynamically changing reference trajectory in real MASS system. Also maneuver path advance dependent on the path tangential angle difference, to ensure trajectory tracking for turns from 0 to 90 degrees, without overshoot is used. All results were obtained with the use of training ship in real–time conditions.

Key words: model predictive control; MPC; ship control; autonomous ship; trajectory tracking; line of sight; LOS.

1. INTRODUCTION

Trajectory tracking is a big challenge for mobile wheeled robots, autonomous cars, autonomous surface ships (ASS), aerial vehicles and unmanned underwater vehicles (UUV). The main goal is to force autonomous vehicle to track a set of waypoints located in the predefined space. It was decided to implement model predictive control (MPC) to the ship trajectory tracking system, because it allows for sub-optimal control signals estimation taking into account ship dynamics, model and output variable constraints and rates, which correspond to real signal limitations.

There are various MPC strategies, which incorporate disturbance model and feed-forward action, which are important when operating in real conditions and minimize their influence on the ship control system performance. Kayacan *et al.* in [1] presented linear MPC incorporating error-based model taking derivative of the error state. They proposed feedforward actions, combined with robust control action, where derivative of the uncertainty vector was considered to reduce overshoots and steady state errors. Kamel *et al.* [2] proposed the low-level attitude controller, combined with model-based trajectory tracking system to steer micro aerial vehicle taking into account its dynamics. They used external disturbance observer and feed-forward term by setting the reference control input in MPC.

In addition to maritime applications, trajectory tracking was used in autonomous vehicles and robots guidance [3]. It may have been combined with linear or nonlinear MPC to deliver efficient guidance law. Baca *et al.* in [4] presented novel approach for optimal trajectory tracking for unmanned aerial vehicles (UAV), where linear MPC was combined with non-linear state feedback. In this concept linear MPC application allowed for fast on board computation and UAV guidance. Fast nonlinear feedback was capable of performing agile maneuvers. This concept also was used in marine applications, as leader-follower [5] and swarm optimization algorithms [6].

Autonomous ship motion control problems consist of two basic issues: safe trajectory generation and trajectory tracking. It may be resolved by application of the nonlinear MPC, where path generation, outputs prediction and sub-optimal control signals computation are realized in one system [7]. Separate safe trajectory generation is similar to mobile robot obstacle avoidance, but vessels with right of way are treated as moving obstacles. Congruent topics are discussed in the publication [8] in relation to mobile nonholonomic robots. Error-based MPC concept, which minimizes output signal errors is described in [9,10]. It leads to the control action guaranteeing lack of steady-state errors.

Trajectory tracking algorithm combines guidance law with automatic control. Line-of-sight (LOS) is a popular and effective guidance algorithm proposed by Fossen *et al.* in [11], where it was used to determine a way back to the ship reference trajectory. It was adopted for parafoil automatic control [12], where bank angle varied proportional to the LOS angle. LOS was combined with optimal control algorithm with bank angle treated as control variable, therefore LOS and MPC in ship trajectory tracking are reasonable.

In conventional LOS algorithm value of the sideslip angle is not taken into account. It leads to the steady state cross-track

*e-mail: a.miller@we.umg.edu.pl

Manuscript submitted 2022-10-03, revised 2023-03-15, initially accepted for publication 2023-04-20, published in August 2023.

error, may cause instabilities in control system and deteriorates overall trajectory tracking performance. Unfortunately in MASS systems environmental disturbances, like wind, waves and currents, causing drift cannot be omitted. Integral LOS (ILOS) [13] is the best-known and most common method of drift angle compensation, but it is applied only for constant sea currents and wind dynamics. Wan *et al*. [14] extended the ILOS method, applying it to time-varying sideslip angle, caused by time-varying disturbances.

Predictor LOS-based (PLOS) guidance law [15] may be applied to any parametric paths. This method is applicable to unmanned surface vessels with unknown dynamics time-varying currents. In this concept yaw rate and surge speed controllers using trajectory linearization control technology are combined with path prediction model providing estimates of unknown sideslip angle caused by ocean currents.

In standard MASS system PID controller is combined with LOS guidance law. To get better performance and control action close to helmsman steering PID is replaced by fuzzy logic controller [16]. Sideslip angle is hard to calculate, but its compensation is crucial. In manual control mode helmsman does not calculate ships drift, but does his best to steer along predefined path. According to this rule model uncertainties and external disturbances are approximated by the adaptive fuzzy system with estimator-based fuzzy updating law.

MASS actuators are constrained in their force, angle of rotation, rudder angle and rate of turn. Taking these constraints at a controller design stage leads to smarter and simpler system. Therefore, the combination of model predictive control (MPC) and LOS has gained popularity. It was introduced by Naeem [17] and used to control reference heading angle of underwater vehicle. Genetic algorithm was used as an optimization tool, to look for an optimal control sequence in each time step. External disturbances and sideslip angle have not been taken into account there. Oh and Sun [18] proposed MPC to render good helmsman behavior during trajectory, defined by set of waypoints (WPT), tracking. LOS algorithm was adopted as a reference trajectory for ship to follow. They used standard criteria of switching to the next straight line segment, when passing current WPT. LOS lookahead distance was added to standard MPC algorithm as a decision variable, to improve path following performance. This concept is applicable only to simulations without disturbances, where future LOS distance may be predicted. Discrete MPC, where rudder is constrained by angle and rate, combined with LOS is used for deterministic path following in [19]. This concept is not applicable to real MASS, because it does not take into account sideslip angle and should not be applied for steering in disturbed environment. Pavlov, Nordahl and Breivik [20] proposed time-varying lookahead distance updated by the MPC algorithm. Hereby they specified acceptable inputs and applied cost function with minimum corresponding to the fast path convergence. In this application MPC was combined with LOS to determine reference LOS angle and feedback linearizing controller was used to track it.

MPC combined with LOS guidance law is commonly used in control systems. They are applicable in space technology for spacecraft rendezvous, where hard constraints are used to maintain trajectory inside safe region and LOS constraints are applied to MPC algorithm [21, 22]. They are also used for curve path following, where LOS gives faster convergence and smaller overshoot [23]. Moreover dynamically reconfigurable constraints are applied to MPC algorithm during spacecraft docking and guidance [24]. In the presented research also similar method was applied in order to incorporate dynamically changing rate of reference rotational velocity change as an MPC constraint.

In underwater vehicles control MPC is frequently used for heading control problem and is combined with virtual guidance LOS, giving high accuracy [25]. It is also applicable for leader-follower control of autonomous underwater vehicles formation, where state constraints are used for collision avoidance [26]. In this publication, authors showed connection of desired optimal heading generation by LOS algorithm with reference governor lack of sway actuator. It was inspiration to use reference rotational speed correction, changing maneuver path advance and approximated rotational speed constraint to bound the increment of desired heading.

MPC-LOS combination is also applicable to the autonomous surface vessels. Where it can deal with collision avoidance rules and is applicable to the distributed control architecture [27]. It may be used for simultaneous ships path following and roll motion control, where actuation amplitude and rate are both limited [28]. LOS is there used for straight line path following and MPC as natural control method for roll constraint enforcement, physical limitation of control inputs and multiple control objectives. Also nonlinear MPC control combined with LOS may be applied to autonomous surface vehicles. In this case relationship between the autonomous vessel and path is combined to get path following error dynamics [29] and therefore tracking problem is transformed into stabilization problem.

Real MASS is guided according to a predefined route consisting of the set of waypoints. Safe trajectory is provided by the superior system with the frequency $f \leq 0.25$ Hz. Therefore, automatic trajectory tracking system should work with a step-changing input and should keep the assumed accuracy. Predictive algorithms, which are counted among model-based control strategies, seem to be useful in the trajectory tracking systems [30].

MPC, with LOS guidance law combination, gives great application possibilities. Ship trajectory return course is determined in a way similar to human steering. Ship to be steered, moving full-ahead, is underactuated, due to no sway force control. Moreover, in this research, during lake trials, ship drift and control signal limitations are taken into account. Therefore, it was decided to use MPC control. It was combined with one of the most mature guidance between two WPT technologies – LOS [29]. These two features show that it is possible to incorporate this control system into real autonomous ship, moving in the disturbed environment, where environmental forces cause ship drift due to uncontrollable sway force applied to the hull. MPC controller has better performance and is less sensitive to the external disturbances than PID [29]. According to the author's knowledge all concepts presented in the literature have to be slightly modified, in order to get a control system for real floating MASS, sailing in a disturbed environment. The discrepancy between mathematical predictive model and the actual ship dynamics should be taken into account. It is hard to get reliable model describing relation between azipod angle of rotation (δ) and ship course (ψ). Identification procedure is complicated, due to initial heading impact on the model output. Therefore mathematical model mapping azipods angle of rotation to rate of turn ($\delta \rightarrow r$) is proposed instead of $\delta \rightarrow \psi$ model. The novelty contained in the work joins usage of the rate of turn (ROT) as a controlled variable in LOS guidance system with r-mapping system design.

With this background, the aim of this paper is to present a workflow during MPC and LOS integration. For this purpose, four issues are described in a detailed way. Training ship (LNG Carrier) and her linearized model are presented in Sections 2.1 and 2.2. 'Dorchester Lady' is treated as a MASS for this research purpose and her linearized model for prediction is presented. MPC–LOS controller, describing model predictive control strategy cooperating with LOS algorithm, involving variable path advance, r-mapping system recalculating responding reference rotational velocity on the basis of LOS return course and current cross-track error are shown in Section 2.5. They are combined with the dynamically changing rotational velocity constraints. Wind action as an external disturbance is described in Section 2.4. In Section 3 results of the real-time lake experiments are presented. Section 4 sums up the research results and presents further research direction.

2. MATERIALS AND METHODS

Maritime Autonomous Surface Ship (MASS) trajectory tracking system which consists of two subsystems: safe trajectory generation and trajectory tracking (Fig. 1) and is based on their cooperation. Second subsystem design, based on cooperation of MPC and LOS algorithms, is the subject of these studies.

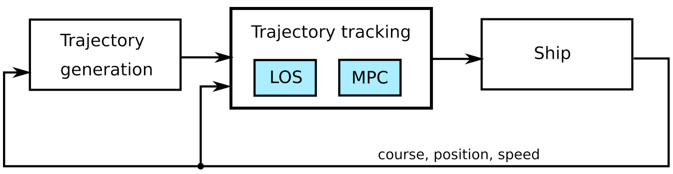

Fig. 1. MASS trajectory tracking system diagram

2.1. The object to be steered

Real floating training ship – LNG carrier is used as an exemplary MASS. LNG carrier "Dorchester Lady" (Fig. 2) is a training ship, built in scale 1:24, owned by Foundation for Safety of Navigation and Environment Protection at the Silm lake near Ilawa in Poland during practical training and research conduction. LNG carrier is equipped with two DC motor-driven counterflow azipods, bow thruster and rotative thruster located on bow. Training ship is a 6DOF object, whose silhouette is presented in Fig. 3. For simulation and control purposes training ship dynamics model is simplified to 3 degrees of freedom

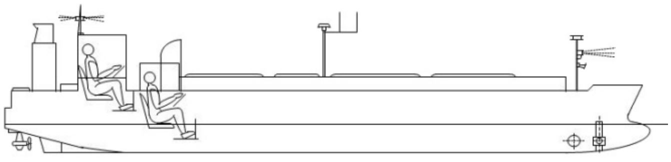

Fig. 2. LNG carrier – 'Dorchester Lady' silhouette [31]

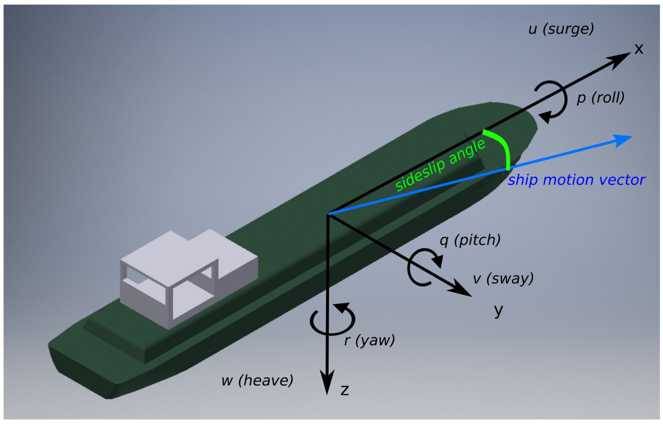

Fig. 3. LNG carrier – 'Dorchester Lady' 3D model

(3 DOF). Due to small waves in the training area, it is considered sufficient to describe surface ship motion, where roll, pitch and heave are omitted.

"Dorchester Lady" is fully actuated ship only during port maneuvers and dynamical positioning. Yaw moment is controlled via azipod rotation, therefore to track 3DOF ship only two controls are available. So this LNG carrier is treated as underactuated one at full-ahead speed, because bow thruster is useful only during maneouvers at low speeds. In autonomous mode ship position is detrmined via DGPS receiver with centimeter accuracy.

Training ship is built according to geometric, kinematic and dynamic similarity laws, with no constant Reynolds number (due to the fact that the ship and model moves in the same environment). This leads to real seagoing ship dynamics mapping. So training ship is a nonholonomic surface vessel having highly non-linear dynamics, moving in disturbed environment, being controlled in real time.

Simplified 3DOF ship dynamics and locating ships local coordinate system origin in the ships center of gravity allows one to describe the dynamics with the following set of equations (1)–(3):

$$m(\dot{u} - rv) = X_{\mathrm{TOT}} \quad [\mathrm{N}], \tag{1}$$

$$m(\dot{v} - ru) = Y_{\mathrm{TOT}} \quad [\mathrm{N}], \tag{2}$$

$$I_z \dot{r} = N_{\mathrm{TOT}} \quad [\mathrm{Nm}], \tag{3}$$

where:

m – ship mass,
I_z – the mass moment of inertia relative to the axis z,
u, v, r – surge, sway, roll

X_{TOT} – total longitudinal force,
Y_{TOT} – total transversal force,
N_{TOT} – total torque.

Assumptions

In order to remain consistent with the ship control theory and simplify and fasten computations in real-time application of the MASS trajectory tracking two assumptions have been made:

Assumption 1. MPC algorithm incorporates identified linear training ships model.

Assumption 2. Trajectory tracking problem is simplified to the path following at operational speed, where reference path is given in a time-free parametrization. There is no need to design a timing law, because ship moves with predefined azipod set-point and her speed decreases only during course change.

2.2. Identified linear model

MPC control scheme needs plant model incorporation. Therefore there is a need to implement a discrete state-space linear one for training ship. Moreover, models task is to predict control signal values in a closed loop, based on past outputs and reference values. Simplification due to Assumption 2 leads to course control while maintaining constant values of propeller revolutions. Specific trajectory point reaching has been made independent of time.

LOS algorithm is used for desired ships course estimation. Therefore, the course (ψ_{LOS}) and propeller angle of rotation (δ_z) are respectively output and control signals in the complete automatic control system. This is applicable for azipod driven ships, which are not equipped with rudder. In view of the above notation, predictive model should map $\delta_z \to \psi_{\mathrm{LOS}}$. But there is a difficulty in such a model identification, because output course values depend on the ships initial course. This problem may be solved in one of two ways: using incremental model (hard to identify) or using model based on angular velocity (r).

It was decided to base on the r value and to replace course of the ship by her angular velocity according to equations (4)–(5):

$$\dot{\boldsymbol{\eta}} = \begin{bmatrix} \cos\psi & -\sin\psi & 0 \\ \sin\psi & \cos\psi & 0 \\ 40 & 0 & 1 \end{bmatrix} \cdot \boldsymbol{\upsilon}, \tag{4}$$

$$\boldsymbol{\upsilon} = \begin{bmatrix} u, & v, & r \end{bmatrix}^T, \quad \boldsymbol{\eta} = \begin{bmatrix} x, & y, & \psi \end{bmatrix}^T, \tag{5}$$

describing 3 DOF nonlinear maneuvering model [11].

Angular velocity is then defined by:

$$r = \mathrm{d}\psi/\mathrm{d}t. \tag{6}$$

Based on the conducted analysis model in the $\delta_z \to r_{\mathrm{LOS}}$ form is identified and used for the future control signal predictions in MPC–LOS controller.

Identification procedure is done using Matlab Identification Toolbox, based on the LNG carriers simulator. It incorporates training ship dynamics mathematical model, which is described in a detailed way in [31, 32]. Description of the test bed was presented in [33]. Pseudo-random signal generator is used as the input signal source – corresponding to azipod angle of rotation. Angular velocity values are recorded and used as output signals during modeling. Verification data is gathered during real-time lake trials. It allows for model uncertainties highlighting and uncertain models removal during iterative identification procedure.

This leads to a model having simple structure, fit for verification data better than 85% for short time predictions (up to 5 seconds) and better than 40% for long time prediction (up to 20 seconds). The assumptions about fit were met for model with structure given by equations (7)–(12):

$$\mathbf{x}_{k+1} = \mathbf{A}\cdot\mathbf{x}_k + \mathbf{B}\cdot\mathbf{u}_k + \mathbf{K}\cdot e_k, \tag{7}$$

$$\mathbf{y}_k = \mathbf{C}\cdot\mathbf{x}_k + e_k, \tag{8}$$

where:

$\mathbf{A},\mathbf{B},\mathbf{C}$ – state, input, output matrix,
$\mathbf{K}$ – noise component matrix,
$\mathbf{u}$, $\mathbf{y}$ – input and output vectors,
$\mathbf{x}$ – state vector,
e – disturbance,
k, $k+1$ – current time, next time moment.

And the particular coefficient values are listed below:

$$\mathbf{A} = \begin{bmatrix} 0 & 1 & 0 & 0 \\ 0 & 0 & 1 & 0 \\ 0 & 0 & 0 & 1 \\ -0.23 & 1.47 & -3.20 & 2.96 \end{bmatrix}, \tag{9}$$

$$\mathbf{B} = \begin{bmatrix} -0.73 \\ -0.66 \\ 1.02 \\ -4.96 \end{bmatrix} \cdot 10^{-4}, \tag{10}$$

$$\mathbf{C} = \begin{bmatrix} 1 & 0 & 0 & 0 \end{bmatrix}, \tag{11}$$

and

$$\mathbf{K} = \begin{bmatrix} 1.71 \\ 2.03 \\ 2.37 \\ 2.67 \end{bmatrix}. \tag{12}$$

Figure 4 illustrates 5-, 10- and 20-step ahead model output predictions compared with verification data. A slightly better fit is achieved than assumed, guaranteeing proper operation of the MPC angular speed controller. Identified model is incorporated to the MPC controller, forming a trajectory tracking system together with line-of-sight algorithm.

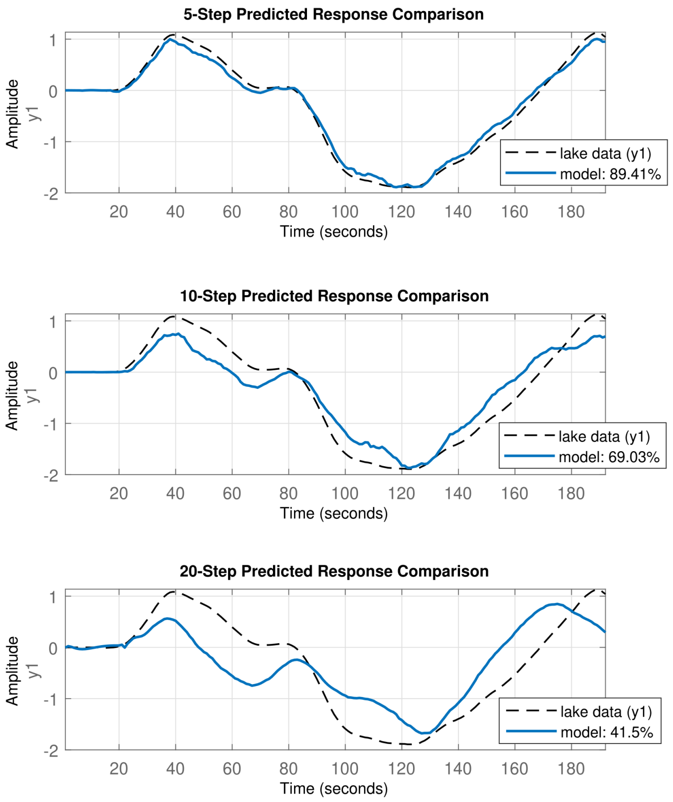

Fig. 4. 5-, 10- and 20-step ahead model output predictions ('model') compared with verification data ('lake data')

2.3. Line-of-sight guidance

Line-of-sight (LOS) ship guidance algorithm, proposed by Fossen *et al.* in [11], is based on the trajectory return course determination. It is one of two mainly used ship positioning relative to a given trajectory methods, apart from relative longitudinal and transversal distance combined with course difference.

LOS method is used in the research due to its simplicity. Its incorporation into MPC control law leads to Single Input Multiple Output (SIMO) or Single Input Single Output (SISO) ship dynamics model identification, respectively depending on whether speed is treated as controlled variable or not. While relative distances approach combined with model-based control strategy leads to multivariable control law, which requires more complicated Multiple Input Multiple Output (MIMO) ship dynamics model and more computing power to ensure systems real-time operation, which is the main reason of its rejection in real time applications. Therefore in this work LOS algorithm is combined with MPC controller to get fast and reliable trajectory tracking system for MASS.

LOS trajectory return course ψ_{LOS}, according to the idea presented in Fig. 5, is determined by cross-track error y_e and lookahead distance (d_{LOS}) linking ships center of gravity with the predefined trajectory. Ship positions (x, y) and waypoints (WPTs) are defined in Earth-fixed coordinate system with x and y pointing North and East respectively. Trajectory return course (ψ_{LOS}) relies on geometrical finding of a point ($x_{\text{LOS}}, y_{\text{LOS}}$) on a given trajectory and setting bearing on it. Trajectory return

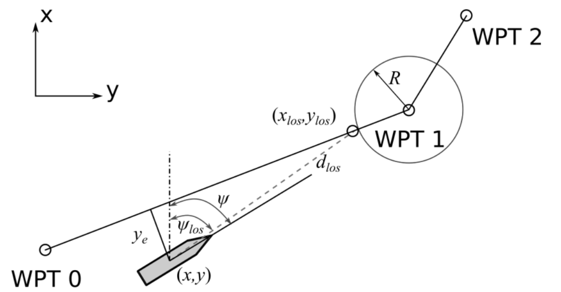

Fig. 5. LOS course definition principle

course [11] is calculated according to equation:

$$\psi_{\text{LOS}} = \operatorname{atan2}\left(y_{\text{LOS}} - y, x_{\text{LOS}} - x\right), \tag{13}$$

where: x, y – current ship position.

Radius R defines maneuver advance – distance from the waypoint where the entrance to the next section of the trajectory begins. In fact this point is defined as intersection of the current trajectory segment with a circle of radius R. For greater accuracy variable length of the maneuver advance may be used. It changes depending on the angle between particular trajectory segments.

2.4. Environmental disturbances

LOS algorithm allows for ship trajectory return course estimation even in the disrupted environment, where sideslip angle is taken into consideration. Ship is exposed to the environmental disturbances, which have to be taken into account during control system design, as a feedforward action, or during trajectory return course estimation. In MASS guidance they are wind, waves and currents. Only in simulations there is a possibility to ignore wind disturbances. Research was done in real lake conditions, where especially wind force has a significant impact on the movement of ship and automatic control system operation. The occurrence of waves disturbing autonomous ship control affects only seas and oceans.

The most common study considers the effects of wind and wave on the ship hull. Wind acts on the ship surface which is above the waterline and its impact strength depends on the ratio of the air resistance area to the hull-force component. LNG carrier "Dorchester Lady" is sensitive to wind due to small draught and high freeboard. Ship behaves differently depending on the relative wind direction:

- **wind from the bow quarter** – causes mainly longitudinal ship speed decrease;
- **amidships wind** – causes ship drift and sideslip angle increase;
- **wind from the aft quarter** – causes mainly yaw moment;
- **wind from the aft** – increases ship longitudinal speed.

Another factor that disturbs ship motion is a current. Moving mass of water affects wetted hull surface. Current action force depends on the draught and ship mass. Ship exposed to current behaves similarly to the ship exposed to wind, according to the apparent current direction.

Training ship MASS trajectory tracking performance was tested only in lake conditions and control system robustness to the external disturbance was proven only by the wind action, which was measured during each trial.

2.5. MPC – LOS controller

LOS and MPC algorithms connection aims to create sub-optimal automatic trajectory tracking system for MASS. Where reference trajectory may change not more often than every 15 seconds during operation due to alternating navigational situation. Presented concept, schematically shown in Fig. 6, demonstrates connections between three elements:

- **LOS algorithm** – takes as inputs set of three waypoints, current ships course and position and calculates ψ_{LOS} trajectory returning course, which guarantees fast and oscillations-free trajectory tracking;
- ***r*-mapping block** – in which trajectory return course and cross-track error values are recalculated to responding reference value of the angular velocity;
- **MPC controller** – estimates sub-optimal control signal values (desired azipod angle of rotation δ_z) based on present and past ships angular velocity values and reference.

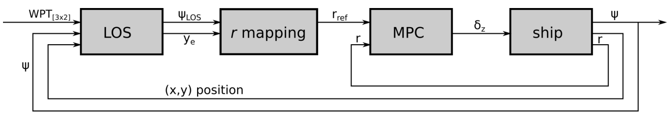

Fig. 6. MPC – LOS controller schematic

Standard LOS algorithm, described by equation (13) and presented in Fig. 5, was used in the designed MASS control system. Ship turn is described by an arc fragment, whose radius depends on the angle of turn. Automatic trajectory tracking system design requires knowledge about the relationship between radius and path-tangential angle of the reference trajectory, which corresponds to angle of turn. Maneuver path advance is defined as a distance to the nearest waypoint, where ship turn should start in order to finish on the next trajectory segment without overshoot. Maneuver path advance is measured during real-time lake experiments for the following path-tangential angles: 25°, 35°, 45°, 60° and 90°. Measured dependence is approximated with polynomials according to the equation:

$$R(\gamma) = 0.0019\gamma^2 + 0.2364\gamma + 0.1696, \tag{14}$$

which is used to extend LOS algorithm and allow for trajectory tracking with minimized overshoot on turns. Approximation results are presented in Fig. 7. Numerical values of coefficients for a polynomial $R(\gamma)$ presented in equation (14) guarantee the best fit of approximated curve to the measured path advance in a least-square sense.

In the r-mapping subsystem LOS-defined reference course (ψ_{LOS}) is converted to the reference rotational velocity (r_{LOS} [deg/s]), being component of the reference signal for MPC controller (r_{ref} [deg/s]). Reference value is corrected using Forward Euler Method:

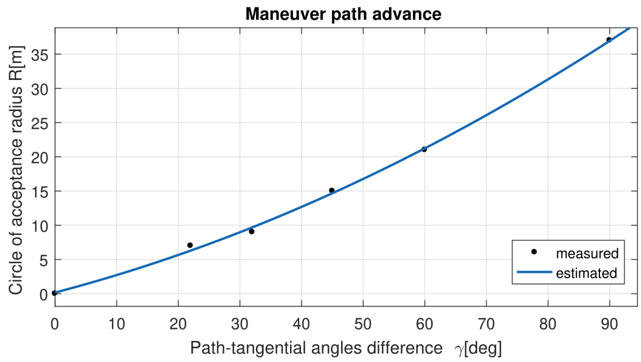

Fig. 7. Maneuver path advance estimation

$$r_{\text{cor}}(k) = \begin{cases} r_{\text{cor}}(k-1) + \dfrac{y_e}{11}[t(k) \\ -t(k-n)]r_{\text{LOS}}(k) & \text{if } |y_e(k)| < 4 \vee \\ & \vee(|r(k)| < 0.3 \wedge \\ & \wedge |y_e(k)| > 4), \\ 0 & \text{else,} \end{cases} \tag{15}$$

where: y_e – cross track error and $t(k) - t(k-n)$ – integration time.

Both rotational velocities are defined according to equations:

$$r_{\text{LOS}} = \frac{\beta(k) + \psi_{\text{LOS}}(k)}{T_s} - \frac{\beta(k-1) + \psi_{\text{LOS}}(k-1)}{T_s}, \tag{16}$$

where: $k-1$ – previous time step, k – current time step, β – estimated sideslip angle, T_s – system sample time, and:

$$r_{\text{ref}} = r_{\text{LOS}} + r_{\text{cor}}. \tag{17}$$

In the proposed method integral action (ILOS) is incorporated into r-mapping subsystem according to equation (16). Time-varying sideslip angle (β) is estimated based on the relative wind speed and direction which are measured by the ultrasonic anemometer installed on board. Presented ILOS is a modified LOS guidance law, where integral actions compensate drifting effect in order not to amplify path following errors due to sideslip angle.

Reference rate of turn value correction (r_{cor}) is arguable only in two cases: for small values of the present cross-track error and for small values of r with simultaneous big cross-track error magnitude. As a small cross-track error we assume values less than two ship breadths. Small value of r is less than 0.15 of the maximum ship rate of turn value. For a LNG carriers they are less than 4m and 0.3°/s for cross-tack error and for r respectively.

Reference rate of turn value correction usage leads to faster operation of the control system without overshoot amplification and whole automatic trajectory system destabilization. Result of applying this solution is an integral action incorporation only in reasonable cases. They are defined as situations in which reference values are small and path convergence is too slow to ensure precise trajectory tracking in dynamically changing reference, which is common in real MASS systems.

LOS algorithm is used as a reference rotational velocity r_{ref} generation system for predictive control system. In the presented training ship MASS trajectory tracking system constrained quadratic programming is used to determine suboptimal control signals. Cost function has a form presented below:

$$J = \gamma_y \sum_{p=N_1}^{N} \left[r_{\text{ref}}(k+p|k) - r(k+p|k)\right]^2 + \gamma_u \sum_{p=0}^{Nu-1} \left[\Delta\delta_z(k+p|k)\right]^2, \tag{18}$$

where: γ_u, γ_y – output signal change and error weight coefficients, r_{ref}, r, $\Delta\delta_z$ – reference, output and control signal change values, $*(k+p|k)$ – signal value at $k+p$ time moment predicted in k time moment, N, N_u – prediction and control horizon lengths.

In conventional MPC scheme control and output signals are constrained by actuator physical limitations and guidance law limits respectively. In the MASS trajectory tracking system azipods angle of rotation (δ_z) is limited to $\pm 20°$, which corresponds to the maximum pod angle of rotation during sea voyage with full ahead speed. Moreover azipods may change their angle of rotation ($\Delta\delta_z$) about $\pm 35°$/s. So control signal constraints are defined as:

$$-20 \le \delta_z \le 20 \ \ [°], \tag{19}$$

$$-35 \le \Delta\delta_z \le 35 \ \ [°/\text{s}]. \tag{20}$$

Instead of linear constraints in standard form, dynamically changing ones are applied for output signal. Ship rate of turn depends on her longitudinal speed, azipod revolutions, angle of rotation, duration of the maneuver and whether azpiods changed their position from one ship side to another. During trajectory tracking training ship moves full-ahead, so simplification of the constraint description has been introduced. It is assumed that ship navigates with constant speed. In fact training ship moves only with constant pod revolutions. But taking into account ship dynamics, revolutions set-point has greater impact than longitudinal speed on the LNG carrier motion. The function describing dynamic constraints is determined for a training ship during real-time trials.

When ship moves full-ahead, azipod angles of rotation should be less or equal to 20°, in order not to damage them. Dynamically changing rate of turn constraint was estimated based on the set of 20 Kempf trials 20/20 at full-ahead. Their results were averaged and function describing relationship between maneuver duration, change in propeller rotation angle sign and rotational speed given by the equation:

$$\begin{aligned} r(t) = {} & 8.381 \cdot exp(-((t+18.51)/56.99)^2) \\ & + 0.6122 \cdot exp(-((t-20.39)/3.869)^2) \\ & - 1.863 \cdot exp(-((t-52.7)/9.233)^2) \\ & - 7.069 \cdot exp(-((t+3.551)/16.28)^2) \\ & - 3.827 \cdot exp(-((t-33.01)/24.9)^2), \end{aligned} \tag{21}$$

was approximated with the use of Gaussian model.

Estimated coefficient values are fit peaks of the Gaussian model. They are given by amplitude, centroid (location) and peak width for each peak. It is assumed that model having square estimate error (SSE) less than 0.25 and root-mean-square error (RMSE) 0.07 is treated as good enough. In order to get Gaussian model meeting the above criteria, model with 5 peaks is used. All coefficients are computed with 95% confidence bounds. Approximation results are presented in Fig. 8. Change in propeller rotation angle sign is indicated by the red vertical lines.

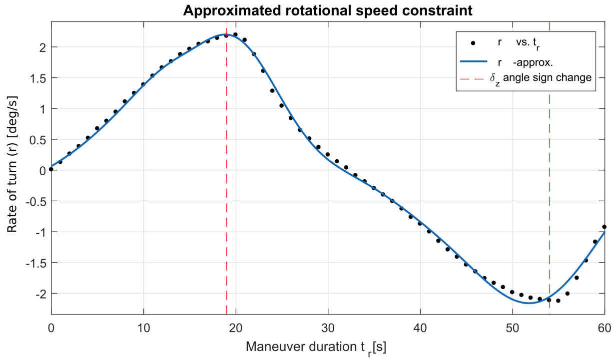

Fig. 8. Approximated rotational speed constraint

Proposed dynamically changing constraints: rate of reference rotational velocity change (Δr_{ref}) and reference maximal value are defined in each time step according to:

$$\Delta r_{\text{ref}} = r(t) \begin{cases} t \in \langle 0, \Delta t_r \rangle & \text{if ship moves along straight line,} \\ t \in \langle 19, \Delta t_r \rangle & \text{if ship turns right,} \\ t \in \langle 54, \Delta t_r \rangle & \text{if ship turns left,} \end{cases} \tag{22}$$

where: Δt_r – maneuver duration. Reference rotational velocity change depends on the desired direction of turn (left/right) and maneuver duration.

In Δr_{ref} three time intervals, describing three separate motion cases, have been defined. They are used for time-varying rotational velocity ($r(t)$) constraint value estimation and are defined based on the mean Kempf test result shown in Fig. 8. Kempf test starts when ship moves with a constant speed and course and this moment is indicated by $t = 0$. First condition in rate of rotational velocity change concerns longitudinal motion preceding ship turn. Therefore the time in equation (22) varies from 0 to whole maneuver duration (Δt_r). Second condition describes turn to starboard side. In equation (22) time t is replaced by a number from 19 to $19 + \Delta t_r$, which is directly related to the change of pod angle of rotation form starboard to port side, shown in Kempf trial (Fig. 8). Third case is analogous to the second one, but is associated with the pod from port to starbaord side rotation, which is observed in 54^{th} second of the motion in Fig. 8.

3. RESULTS

LOS–MPC controller was verified in real lake conditions and results of these experiments are presented in Figs. 21–26. LNG carrier "Dorchester Lady" training ship was used as a plant.

Safe trajectory was generated via master subsystem not more often than every 15 seconds. Two types of tests were carried out:

- static tests – during which one predefined trajectory was sent to the control system and it was tracked during a particular trial;
- dynamic tests – where ship was tracking dynamically generated trajectory, which corresponds to the real, changing navigation situation.

In static tests, it is assumed that cross-track error in steady state is less than half ship breadth and on turns it is less than 1–2 ship breadths, which is respectively equal to $y_e \leq |0.9|$ [m] and $y_e \leq |3.8|$ [m] for the training ship. Oscillations in steady state trajectory are not acceptable in real MASS system. Five static tests were carried out. They illustrate the impact of including maneuver path advance (MPA), integral action via reference value correction (r_{cor}) and introduction of dynamically changing constraints ($r(t)$) on the quality of control. Results for all trials are presented in the same scheme. In three figures, generated for each trial, are presented: realized trajectory compared with the reference trajectory, control and output signals and cross-track error (with the red line marked accepted range of volatility). Moreover wind speed measurements are also included. This figure shows scale of measured external disturbances, impossible to eliminate, acting on the ship. Ship model is moving 1.6m/s full-ahead and wind speed is greater than 2.0 m/s, so it has a significant impact on the ships motion.

First test illustrates trajectory tracking without integral action, MPA and dynamically changing constraints. Results are presented in Figs. 9–11.

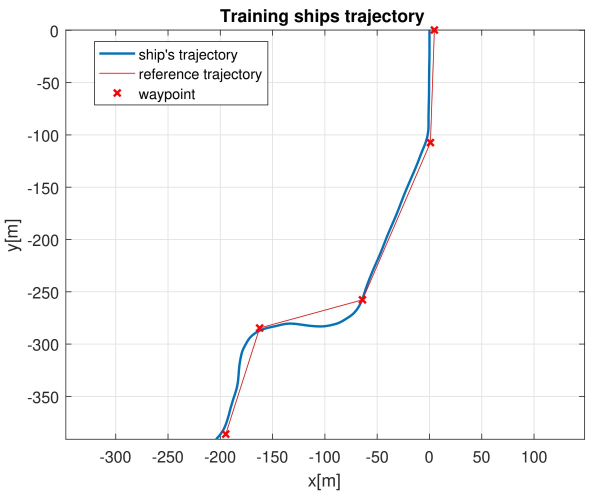

Fig. 9. Training ship trajectory – first static test result

In Fig. 9 ship and reference trajectories do not overlap. Moreover for turns exceeding 45° ship significantly moves away from the reference trajectory. Figure 11 shows occurrence of the steady state error, greater than ship breadth. In turns greater than 45° ship moves away from the reference trajectory for more than 10 ship breadths. Moreover, as the wind force increases, the energy expenditure necessary to keep the ship on its trajectory increases. MPC controller shows robustness to the wind action, but azipod angle of rotation necessary to keep trajectory tracking increases, which is shown between 200 and 250 s of the experiment in Fig. 10 and Fig. 11, where azipod angle of rotation remains in saturation guaranteed by the control signal constraint compliance. MPC control becomes a case of two-position control, which is ineffective in the case of ship course maintenance. Despite the large energy expenditure associated with the maximum amplitude of thruster deflection, the cross-track error is large and significantly exceeds 10 m, which is unacceptable. Therefore usage of the MPC–LOS strategy without inertial action, MPA in dynamic constraints is unacceptable for MASS.

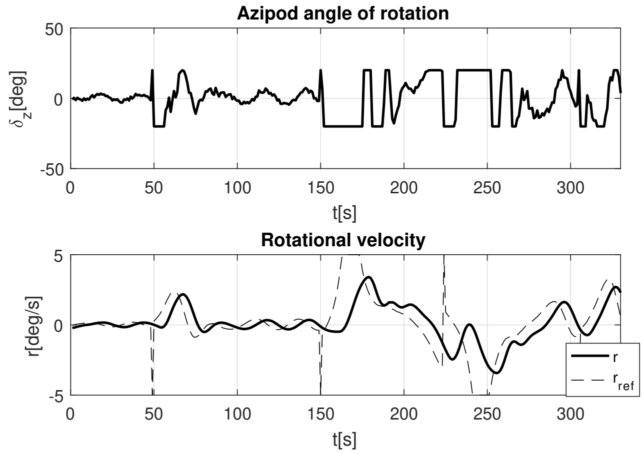

Fig. 10. Control and output signals – first static test result

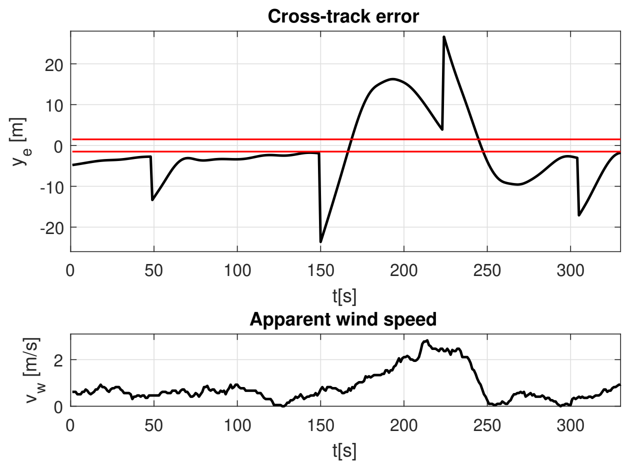

Fig. 11. Cross-track error and external disturbance (wind speed) – first static test result

Second test presents results of trajectory tracking, taking into account integral action. It is realized by reference value correction (r_{cor}) addition in the r-mapping subsystem. Results are presented in Figs. 12–14. This trial was done in heavy wind conditions. Average apparent wind was twice as fast as the speed of the ship. In order to track predefined trajectory MPC controller generated rugged control signal – azipod angle of rotation (Fig. 13).

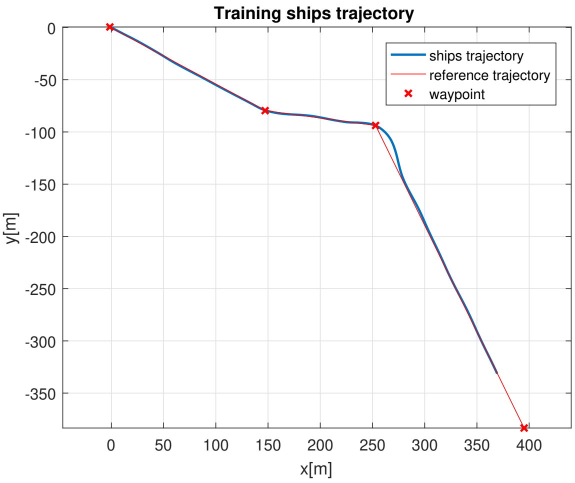

Fig. 12. Training ship trajectory – second static test result

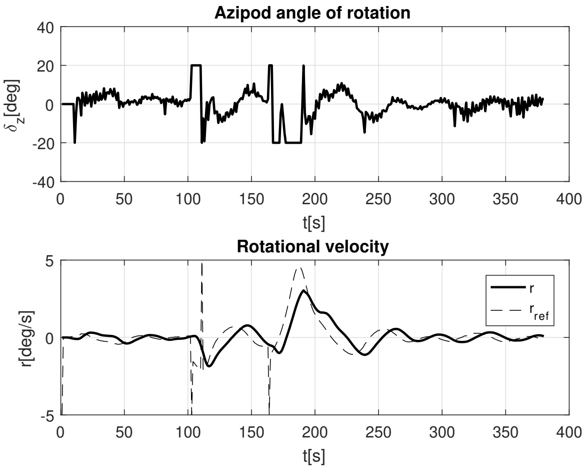

Fig. 13. Control and output signals – second static test result

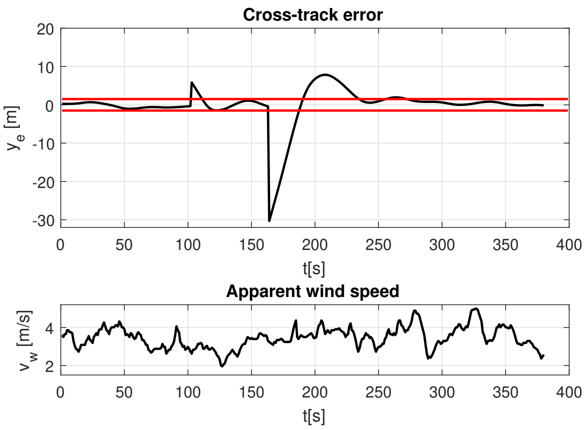

Fig. 14. Cross-track error and external disturbance (wind speed) – second static test result

Integral action incorporation leads to cross-track error minimization and energy expenditure on azipods turning reduction. In Fig. 13 saturation appears only on turns. Analysis of the cross-track error, presented in Figs. 12 and 14, allows us to conclude that there are problems only with the next trajectory section entrance after turn. Beyond the turn and back on the trajectory period (160–240 s of the trial), cross-track error is minimized to the assumed permissible values. So, integral action incorporation significantly improves the quality of trajectory tracking and it is reasonable to incorporate it into MPC–LOS algorithm.

In real MASS system ship drift angle may not be omitted. Its occurrence, combined with finite accuracy of the propellers setting leads to errors in line-of-sight trajectory return course tracking. Integral action, described by equation (15), leads to better trajectory tracking with the lack of steady state error. In the second test MPA is not integrated into control algorithm. So trajectory tracking on turns greater than 45° is unacceptable and ship moves away from the trajectory by about 5 ship breadths. It is presented in Fig. 14 after turn in 200th second of the trial. Moreover after bigger ship turns reference velocity oscillates, which is presented in Fig. 13 and leads to oscillations in the logged ship trajectory.

In the third test variable maneuver path advance is taken into consideration. Trial is conducted with MPA, but without integral action and dynamically changing constraints. Results are presented in Figs. 15–17.

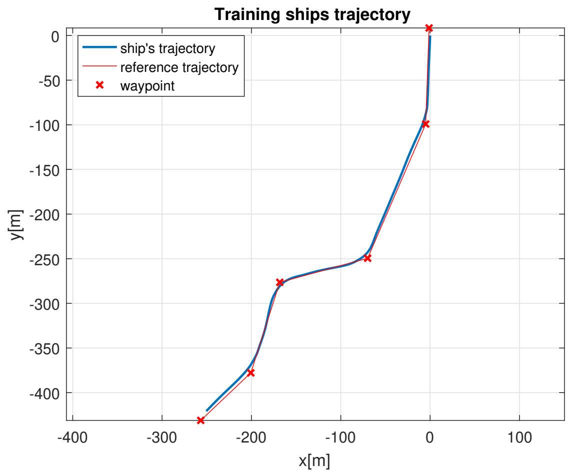

Fig. 15. Training ship trajectory – third static test result

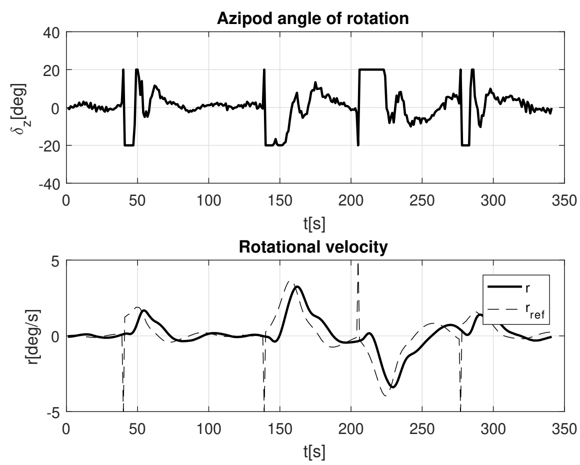

Fig. 16. Control and output signals – third static test result

Fig. 17. Cross-track error and external disturbance (wind speed) – third static test result

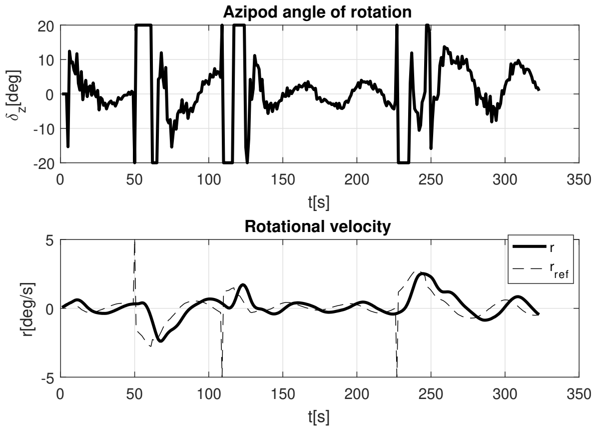

Fig. 19. Control and output signals – fourth static test result

Taking MPA into account leads to better trajectory tracking on turns, due to ship dynamics and maneuvering characteristics incorporation. In most analyzed cases ship after turn returns to the trajectory segment without overshoot. There are no oscillations in cross-track error (Fig. 17), but steady state error occurs due to lack of integral action. Despite the occurrence of the cross-track error between 100 and 140 s of the trial, azipod angle of rotation and reference rotational velocity are close to zero (Fig. 16). Due to lack of oscillations and presence of cross-track error at the permissible limit, trajectory tracking may be treated as satisfactory for MASS. But when comparing with the second test results, it is clear that better results may be obtained by including integral action.

Fourth test shows results of the inertial action and variable MPA incorporation into trajectory tracking algorithm. Only dynamically changing constraints are not taken into account. Results are presented in Figs. 18–20.

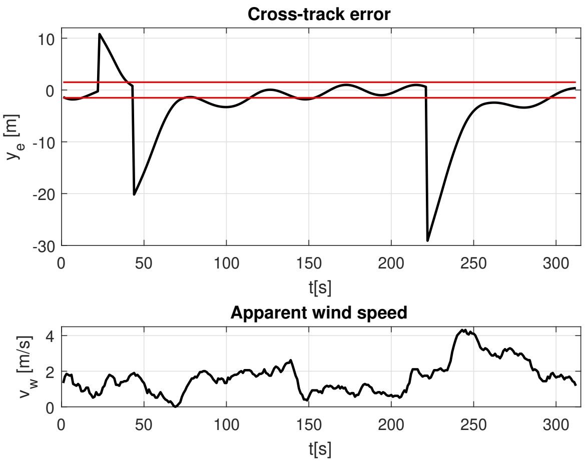

Fig. 20. Cross-track error and external disturbance (wind speed) – fourth static test result

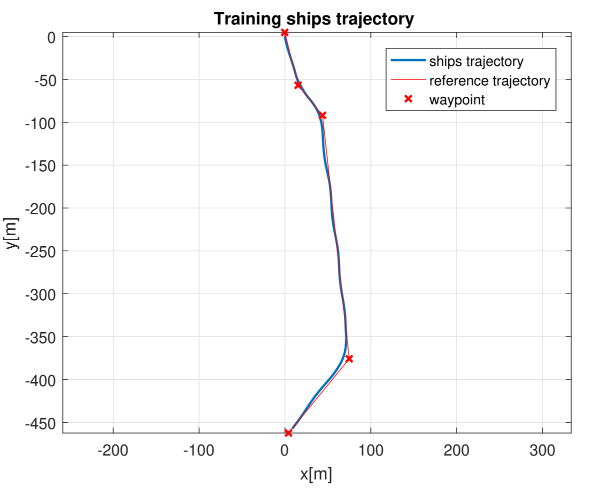

Fig. 18. Training ship trajectory – fourth static test result

In this concept steady state error in cross-track error (Fig. 20) and transversal drift form trajectory after turns (Fig. 18) are eliminated. Cross-track error remains within a predefined limits, so it may be concluded that the assumptions about the quality of trajectory tracking are met. But, when moving along the trajectory segment, treated as steady-state motion, ship course alters. There are seen oscillations with a period equal to 50 s in cross-track error, reference rotational velocity and azipod angle of rotation (Fig. 19, Fig. 20). They are caused by the lack of dynamically changing constraints on rotational velocity. In this case the reference signal rate of change is not related to the vessel dynamics, so unreasonable values of this signal are computed. Plants inertia does not allow for proper reference tracking, which causes oscillations. Despite they are within the permissible cross-track error marked by red lines in Fig. 20, they deteriorate automatic trajectory tracking quality, increase energy expenditure on control and should be suppressed.

Figures 21–23 present exemplary trajectory tracking results for complete MPC ship trajectory tracking system based on LOS method. In the presented algorithm inertial action, dynamically changing constraints and variable MPA are incorporated.

Figure 21 shows that training ship moved along reference trajectory without oscillations and overshoot on turns. This indicates that internal MPC model has good fit to the ship dynamics

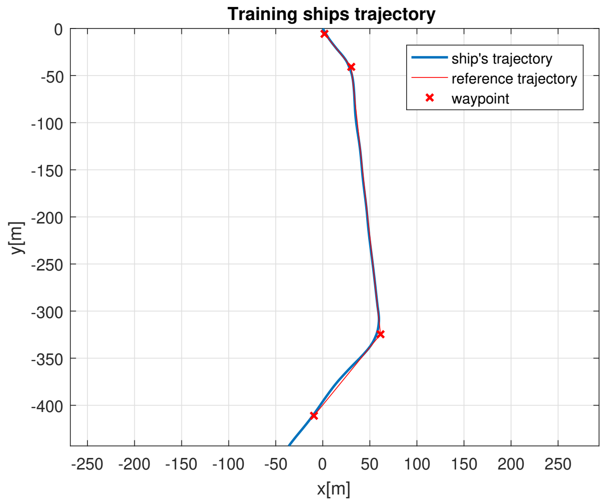

Fig. 21. Training ship trajectory – fifth static test result

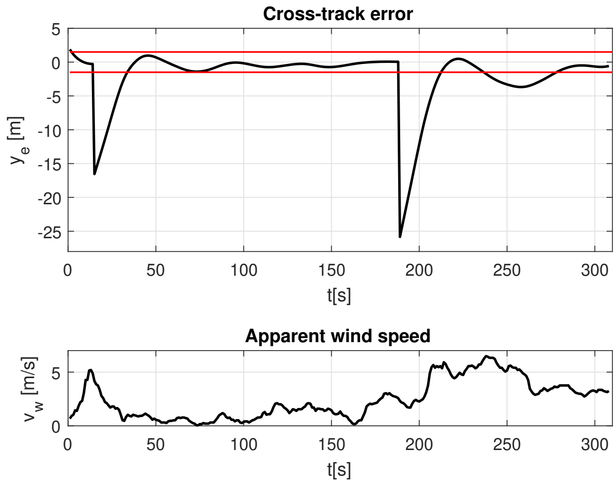

Fig. 23. Cross-track error and external disturbance (wind speed) – fifth static test result

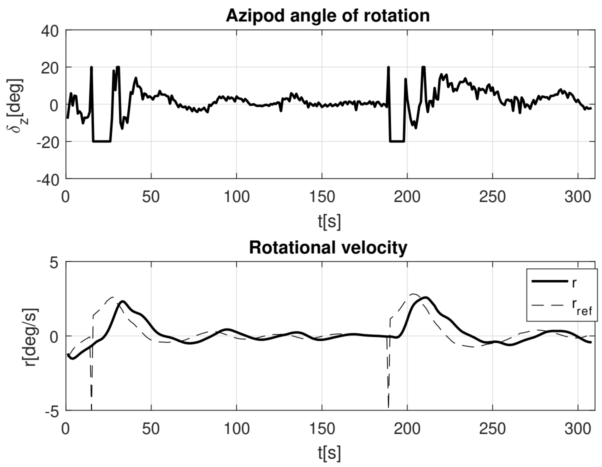

Fig. 22. Control and output signals – fifth static test result

and dynamically changing constraints are approximated properly. Figure 22 presents control (δ_z), reference (r_{ref}) and output (r) signal time trials. In Fig. 23 results of cross-track error and apparent wind speed measurements have been summarized. Cross-track error exceeds the defined range when training ship turns, the reason for which is the method of deviation from the trajectory determination. At the time of the WPT switch, the ship is at a certain distance from it, and the cross-track error is counted as the distance from the new trajectory segment. There is a clear correlation between oscillations in cross-track error, and the occurrence of external disturbance – gusts of wind ($t > 200$ in Fig. 23). After ships turn, between 225^{th} and 275^{th} second of motion, departure from the predefined trajectory, shown as a cross-track error exceeding defined limit (marked by red line in Fig. 23) is due to impact of apparent wind of more than 5 m/s acting on ship. Wind with a force significantly exceeding operating speed of ship (about 1.1 m/s) is a major disturbance, whose impact cannot be omitted. Moreover, it is difficult to be minimized without feed-forward action, based on the wind turbulence prediction. Results of the all test trials are summarized in Table 1.

Having acceptable MPC-LOS controller working in steady state conditions dynamical tests are done. Data is logged during real MASS control. In above mentioned tests four ships are navigating on the Silm Lake. Two of them are forced to keep constant course and speed and the other two are navigating as MASSs. Superior system is generating safe route for each autonomous ship every 15 seconds. Three cases were possible: previously generated trajectory is preserved, new trajectory is delivered to the ship control system, last minute maneuver is realized due to lack of safe trajectory generation possibility.

Table 1
Test results summary

Test No.	inertial action r_{cor}	MPA	dynamic constr. $r(t)$	trajectory tracking for $\Delta\psi_{\text{LOS}} \geq 45°$	trajectory tracking for $\Delta\psi_{\text{LOS}} < 45°$	Y_{ese} steady state error	Y_{eosc} oscillations
Test 1	✗	✗	✗	$Y_e > 10$ ship breadths	about 1 ship breadth	$Y_{ese} > 1$ ship breadth	no oscillation
Test 2	✓	✗	✗	$1 < Y_e < 5$ ship breadths	$Y_e < 1$ ship breadth	no Y_{ese}	$Y_{eosc} < 1$ ship breadth
Test 3	✗	✓	✗	$Y_e \in <1;2>$ ship breadths	$Y_e < 1$ ship breadth	$Y_{ese} > 1$ ship breadth	no oscillation
Test 4	✓	✓	✗	about 1 ship breadths	$Y_e < 1$ ship breadth	no Y_{ese}	about 1 ship breadths
Test 5	✓	✓	✓	$Y_e \in <1;2>$ ship breadths	$Y_e < 1$ ship breadth	no Y_{ese}	no oscillation

In dynamic tests training ship most of her motion time is in turning mode, which is presented in Fig. 24 "Rotational velocity". Therefore there is no reason to define steady-state cross-track error and determine design assumptions fulfillment. Exemplary dynamic test trajectory (Fig. 24) shows, that during experiment lasting 250 seconds, reference trajectory changes 18th times. Ship has to track dynamically changing route. Also angle between successive segments of the trajectory (called "Trajectory course"), which is is treated in the system as a reference course, is presented. It is characterized by high dynamics change, which is associated with output signal overshoots and quite long settling time.

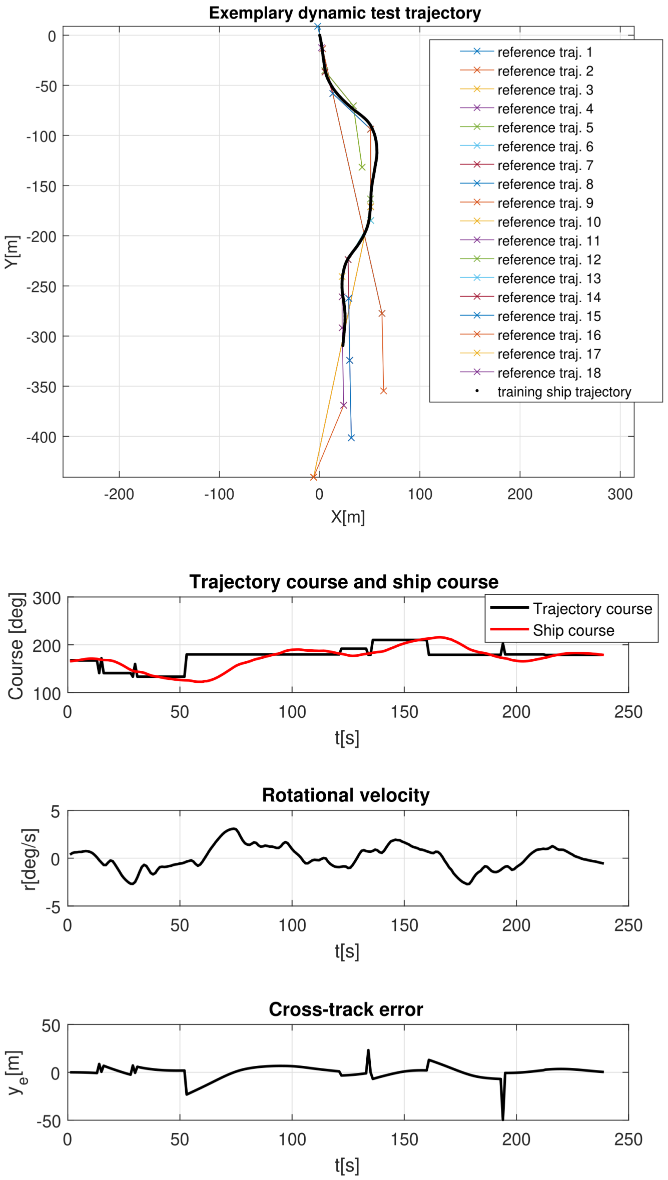

Fig. 24. Trajectory, course, rotational velocity and cross–track error – dynamic test result

For longer straight trajectory segments, cross–track error minimization and rotational velocity decrease are observed (Fig. 24). Difference between trajectory course and ship course is minimized. Convergence of the reference and ship trajectories is also seen. Automatic controller behavior in dynamic tests is found to be correct, because all ship maneuvers have been carried in a logical and safe way. Nowadays it is a main measure of MASS behavior, due to lack of special law rules and regulations for autonomous ships.

Figures 25 and 26 are zoomed slices of the Fig. 24 and show dynamic test results in a detailed way. Figure 25 presents separately individual sections of the trajectory, generated one by one during the maneuver presented in Fig. 24, grouped in pairs. First trajectory consists of two waypoints, constructing straight line segment, which coincides with the first segment of second trajectory. In second trajectory third waypoint forces the vessel to change her course at a later stage of navigation. These two trajectories are generated in 1st and 16th second of ships motion. In 31st second of motion ship is forced to change her course definitely. And third trajectory is delivered by the anti-collision system. Figure 26 presents dependency between trajectory and ship courses, compared with rotational velocity and cross-track error.

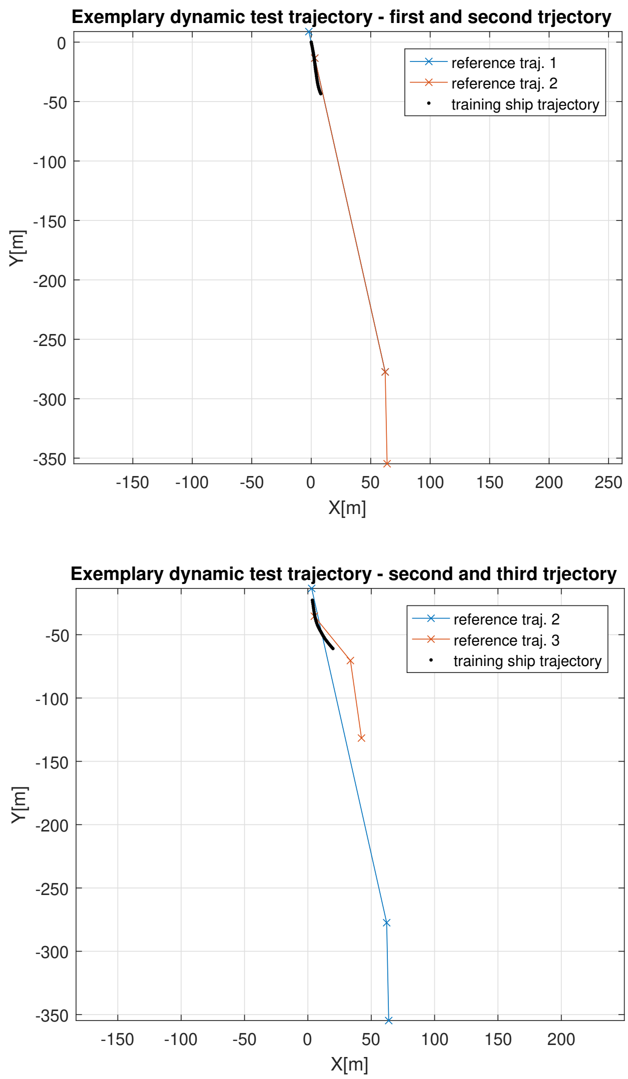

Fig. 25. Exemplary three trajectories generated during dynamic test: upper – first and second, lower – second and third

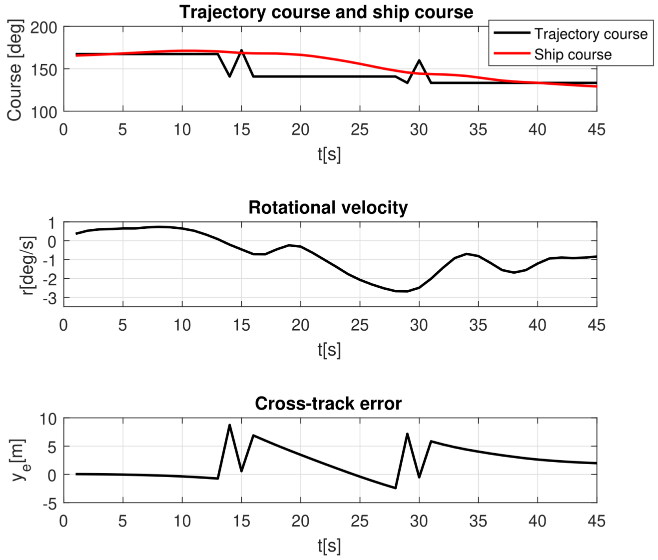

Fig. 26. Course, rotational velocity and cross–track error for the first three trajectory segments – dynamic test result

4. CONCLUSIONS

MPC control and LOS trajectory tracking algorithm were merged and gave fully operational ships automatic trajectory tracking system, which may be directly applied to MASS. It was decided to use such a solution in order to cooperate with the superior safe trajectory generation system. During this cooperation trajectory was adjusted every 15–45 seconds. Therefore ship was turning for the most of her motion and timing control law cannot have been used due to longitudinal speed drop during maneuvers. So in all dynamic tests conducted during presented research MPC-LOS controller was applied to real MASS system. Results were analyzed and their correctness was assessed based on the logical and safe ship behavior empirically. There are no standard mathematical measures to assess control ability during fast changing trajectory tracking.

Variable maneuver path advance usage allows for spline trajectory tracking without overshoot after turn. The angle between trajectory individual sections should change from 0° to 90°. This allows for particular ship circulation radius consideration during control law design. So, method of rotational velocity determination based on the desired trajectory return course was developed, presented and used in real lake tests. Ships angular velocity change was separated from the current ships course and associated with the rotation duration. Therefore there was no need to create a complex predictive incremental model describing course changes. This approach fastened MPC design process, online computations and reduced controller complexity. Rotational speed as a function of the maneuver duration was implemented as a dynamic rate of turn constraint. Its implementation increased trajectory tracking accuracy and minimized overshoot in controlled variable due to reference rotational speed changes corresponding to the ships turning possibilities. Results showed that it significantly improved trajectory tracking performance and allowed for controller cooperation with fast changing reference trajectory generation systems.

New concept of the dynamically changing MASS trajectory tracking system was presented. All concepts were tested under normal MASS operational conditions during real lake trials conducted on training ship “Dorchester Lady”. Controller was built on the basis of Fossen LOS algorithm combined with MPC. Dynamically changing trajectory tracking was a big challenge for automatic control, due to discontinuous and changing with unknown frequency reference. In practice, this has led to situation, where ship being in turn has to track new trajectory. In the worse case ship was in turn to the port side and new trajectory required her turn to the starboard side. Presented new concept allowed for control signals estimation due to dynamically changing rotational speed constraint. Controller “had knowledge” about the minimal maneuver duration and required, changing every time step, rate of turn. Therefore presented MASS trajectory tracking system may be applied to the real MASS in the highest, fourth degree of autonomy, where reference trajectory is given by the safe trajectory generation system in which new trajectories are generated more often than in manual control, which is confirmed by positive results of dynamic tests.

Novel approach to integral LOS action was presented. Error signal integration was conducted only when control signal convergence to reference was slow or impossible to obtain.

Developed MPC-LOS algorithm operates with dynamically changing rotational velocity constraints. They are combined with a variable maneuver path advance leading to good trajectory tracking on turns and integral action built in reference correlation. Future work on the proposed MASS control system will cover curve trajectory prediction and its incorporation into MPC controller as a predicted reference.

REFERENCES

[1] E. Kayacan, H. Ramon, and W. Saeys, “Robust trajectory tracking error model-based predictive control for unmanned ground vehicles,” *IEEE/ASME Trans. Mechatron.*, vol. 21, no. 2, pp. 806–814, 2015.
[2] M. Kamel, M. Burri, and R. Siegwart, “Linear vs nonlinear mpc for trajectory tracking applied to rotary wing micro aerial vehicles,” *IFAC-PapersOnLine*, vol. 50, no. 1, pp. 3463–3469, 2017.
[3] A. Ratajczak, “Trajectory reproduction and trajectory tracking problem for the nonholonomic systems,” *Bull. Pol. Acad. Sci. Tech. Sci.*, vol. 64, no. 1, pp. 63–70, 2016, doi: 10.1515/bpasts-2016-0008.
[4] T. Baca, D. Hert, G. Loianno, M. Saska, and V. Kumar, “Model predictive trajectory tracking and collision avoidance for reliable outdoor deployment of unmanned aerial vehicles,” in *2018 IEEE/RSJ International Conference on Intelligent Robots and Systems (IROS)*. IEEE, 2018, pp. 6753–6760.
[5] W. Kowalczyk and K. Kozłowski, “Trajectory tracking and collision avoidance for the formation of two-wheeled mobile robots,” *Bull. Pol. Acad. Sci. Tech. Sci.*, pp. 915–924, 2019.
[6] V. Kumar and J. Jerome, “An adaptive particle swarm optimization algorithm for robust trajectory tracking of a class of under actuated system,” *Arch. Electr. Eng.*, vol. 63, no. 3, 2014.
[7] T.P. Nascimento, C.E.T. Dórea, and L.M.G. Gonçalves, “Nonlinear model predictive control for trajectory tracking of nonholonomic mobile robots: A modified approach,” *Int. J. Adv. Robot. Syst.*, vol. 15, no. 1, pp. 1–14, 2018.

[8] J. Zhang, S. Zhang, and R. Gao, "Discrete-time predictive trajectory tracking control for nonholonomic mobile robots with obstacle avoidance," *Int. J. Adv. Robot. Syst.*, vol. 16, no. 5, pp. 17–29, 2019.

[9] M. Seyr and S. Jakubek, "Mobile robot predictive trajectory tracking," in *ICINCO*, 2005, pp. 112–119.

[10] G. Klancar and I. Skrjanc, "Predictive trajectory tracking control for mobile robots," in *2006 12th International Power Electronics and Motion Control Conference*. IEEE, 2006, pp. 373–378.

[11] T.I. Fossen, M. Breivik, and R. Skjetne, "Line-of-sight path following of underactuated marine craft," *IFAC Proc. Vol.*, vol. 36, no. 21, pp. 211–216, 2003.

[12] N. Murali, M. Dineshkumar, K.W. Arun, and D. Sheela, "Guidance of parafoil using line of sight and optimal control," *IFAC Proc. Vol.*, vol. 47, no. 1, pp. 870–877, 2014.

[13] W. Caharija, K.Y. Pettersen, J.T. Gravdahl, and E. Børhaug, "Integral los guidance for horizontal path following of underactuated autonomous underwater vehicles in the presence of vertical ocean currents," in *2012 American Control Conference (ACC)*. IEEE, 2012, pp. 5427–5434.

[14] L. Wan, Y. Su, H. Zhang, B. Shi, and M.S. AbouOmar, "An improved integral light-of-sight guidance law for path following of unmanned surface vehicles," *Ocean Eng.*, vol. 205, p. 107302, 2020.

[15] B. Qiu, G. Wang, and Y. Fan, "Predictor los-based trajectory linearization control for path following of underactuated unmanned surface vehicle with input saturation," *Ocean Eng.*, vol. 214, p. 107874, 2020.

[16] J. Nie and X. Lin, "Improved adaptive integral line-of-sight guidance law and adaptive fuzzy path following control for underactuated msv," *ISA Trans.*, 2019.

[17] W. Naeem, "Model predictive control of an autonomous underwater vehicle," in *Proc. UKACC Conference on Control*. Citeseer, 2002, pp. 19–23.

[18] S.-R. Oh and J. Sun, "Path following of underactuated marine surface vessels using line-of-sight based model predictive control," *Ocean Eng.*, vol. 37, no. 2-3, pp. 289–295, 2010.

[19] M. Li, T. Li, Q. Shan, and H. Xv, "Line-of-sight based predictive control for curve path following of underactuated vessels," in *2018 Ninth International Conference on Intelligent Control and Information Processing (ICICIP)*. IEEE, 2018, pp. 122–127.

[20] A. Pavlov, H. Nordahl, and M. Breivik, "Mpc-based optimal path following for underactuated vessels," *IFAC Proc. Vol.*, vol. 42, no. 18, pp. 340–345, 2009.

[21] K. Dong, J. Luo, and D. Limon, "A novel stable and safe model predictive control framework for autonomous rendezvous and docking with a tumbling target," *Acta Astronaut.*, vol. 200, pp. 176–187, 2022, doi: 10.1016/j.actaastro.2022.08.012.

[22] L. Ravikumar, N.K. Philip, R. Padhi, and M.S. Bhat, "Autonomous terminal maneuver of spacecrafts for rendezvous using model predictive control," in *2016 Indian Control Conference (ICC)*, 2016, pp. 72–78, doi: 10.1109/INDIANCC.2016.7441108.

[23] S. Zhao, X. Wang, D. Zhang, and L. Shen, "Model predictive control based integral line-of-sight curved path following for unmanned aerial vehicle," in *AIAA Guidance, Navigation, and Control Conference*, 2017, p. 1511.

[24] A. Weiss, I. Kolmanovsky, M. Baldwin, and R.S. Erwin, "Model predictive control of three dimensional spacecraft relative motion," in *2012 American Control Conference (ACC)*. IEEE, 2012, pp. 173–178.

[25] B. Ma, K. Zhan, Z. Yu, and F. He, "Path tracking control of uuv based on los-mpc decoupling control," in *Proceedings of 2021 International Conference on Autonomous Unmanned Systems (ICAUS 2021)*, M. Wu, Y. Niu, M. Gu, and J. Cheng, Eds. Singapore: Springer Singapore, 2022, pp. 769–780.

[26] Z. Qian, W. Lyu, Y. Dai, and J. Xu, "A consensus-based model predictive control with optimized line-of-sight guidance for formation trajectory tracking of autonomous underwater vehicles," *J. Intel. Robot. Syst.*, vol. 106, no. 1, pp. 1–13, 2022.

[27] Z. Du, R.R. Negenborn, and V. Reppa, "Colregs-compliant collision avoidance for physically coupled multi-vessel systems with distributed mpc," *Ocean Eng.*, vol. 260, p. 111917, 2022, doi: 10.1016/j.oceaneng.2022.111917.

[28] C. Liu, J. Sun, and Z. Zou, "Integrated Line of Sight and Model Predictive Control for Path Following and Roll Motion Control Using Rudder," *J. Ship Res.*, vol. 59, no. 02, pp. 99–112, 06 2015, doi: 10.5957/jsr.2015.59.2.99.

[29] Z. Tian, H. Zheng, and W. Xu, "Path following of autonomous surface vehicles with line-of-sight and nonlinear model predictive control," in *2021 6th International Conference on Transportation Information and Safety (ICTIS)*, 2021, pp. 1269–1274, doi: 10.1109/ICTIS54573.2021.9798580.

[30] W. Gierusz and A. Miller, "Ship motion control system for replenishment operation," *Appl. Mech. Mater.*, vol. 817, pp. 214–222, 2015.

[31] W. Gierusz, "Simulation model of the lng carrier with podded propulsion part 1: Forces generated by pods," *Ocean Eng.*, vol. 108, pp. 105–114, 2015.

[32] W. Gierusz, "Simulation model of the lng carrier with podded propulsion, part ii: Full model and experimental results," *Ocean Eng.*, vol. 123, pp. 28–44, 2016.

[33] M. Rybczak and A. Rak, "Prototyping and simulation environment of ship motion control system," 2019, poster form TransNav 2019 Poster Session, article waiting for publication in TransNav Journal.